MNRAS 000, 1–6 (2017) Preprint 16 March 2022 Compiled using MNRAS LATEX style file v3.0

On the physical mechanisms governing the cloud lifecycle in the Central Molecular Zone of the Milky Way

S. M. R. Jeffreson[1⋆], J. M. D. Kruijssen[1], M. R. Krumholz[2] and S. N. Longmore[3]
[1]*Astronomisches Rechen-Institut, Zentrum für Astronomie der Universität Heidelberg, Mönchhofstraße 12-14, 69120 Heidelberg, Germany*
[2]*Research School of Astronomy & Astrophysics, Australian National University, Canberra, ACT 2611, Australia*
[3]*Astrophysics Research Institute, Liverpool John Moores University, 146 Brownlow Hill, Liverpool L3 5RF, UK*

Accepted 2018 May 1. Received 2018 April 9; in original form 2018 January 23.

arXiv:1805.02655v1 [astro-ph.GA] 7 May 2018

ABSTRACT

We apply an analytic theory for environmentally-dependent molecular cloud lifetimes to the Central Molecular Zone of the Milky Way. Within this theory, the cloud lifetime in the Galactic centre is obtained by combining the time-scales for gravitational instability, galactic shear, epicyclic perturbations and cloud-cloud collisions. We find that at galactocentric radii $\sim$ 45-120 pc, corresponding to the location of the '100-pc stream', cloud evolution is primarily dominated by gravitational collapse, with median cloud lifetimes between 1.4 and 3.9 Myr. At all other galactocentric radii, galactic shear dominates the cloud lifecycle, and we predict that molecular clouds are dispersed on time-scales between 3 and 9 Myr, without a significant degree of star formation. Along the outer edge of the 100-pc stream, between radii of 100 and 120 pc, the time-scales for epicyclic perturbations and gravitational free-fall are similar. This similarity of time-scales lends support to the hypothesis that, depending on the orbital geometry and timing of the orbital phase, cloud collapse and star formation in the 100-pc stream may be triggered by a tidal compression at pericentre. Based on the derived time-scales, this should happen in approximately 20 per cent of all accretion events onto the 100-pc stream.

Key words: Galaxy: centre — stars: formation — ISM: clouds — ISM: evolution — ISM: kinematics and dynamics — galaxies: ISM

1 INTRODUCTION

The Central Molecular Zone (CMZ) of the Milky Way contains the largest concentration of high-density molecular gas in the Galaxy (Ferrière et al. 2007). Despite this large gas reservoir, coupled with high gas pressures and velocity dispersions (e.g. Oka et al. 2001), the observed star formation rate (SFR) in the CMZ is 10-100 times lower than that predicted by standard star formation relations (Yusef-Zadeh et al. 2009; Immer et al. 2012; Longmore et al. 2013a; Kauffmann et al. 2013; Barnes et al. 2017). Galactic dynamical processes appear to play a dominant role in driving the evolution of the high-density clouds. This is supported by a growing body of observational evidence that star formation in the '100-pc stream' of gas at galactocentric radii of $\sim$ 100 pc may be triggered by a tidal compression event, either at the pericentre of an eccentric orbit (Longmore et al. 2013b; Rathborne et al. 2014; Kruijssen et al. 2015; Henshaw et al. 2016b) or due to the change of the gravitational potential during accretion onto the inner CMZ (Kruijssen et al. 2018). The global gas properties of the CMZ can be successfully reproduced by large-scale gas flows driven towards the central supermassive black hole (SMBH) by a combination of gravitational and acoustic instabilities, driving an episodic cycle of large-scale star formation and quiescence (Kruijssen et al. 2014; Krumholz & Kruijssen 2015; Krumholz et al. 2017). The CMZ therefore presents a nearby example of the interplay between galactic dynamics, large-scale gas flows, the feeding of a central SMBH, star formation, and feedback. Its gas reservoir has similar properties to those observed in high-redshift galaxies (Kruijssen & Longmore 2013), such that an understanding of the baryon cycle in our Galactic centre may also shed light on extragalactic star formation.

Throughout the Galaxy, giant molecular clouds (GMCs) host the majority of star formation (Kennicutt & Evans 2012). In order to understand the baryon cycle in the CMZ, it is therefore necessary to understand its cloud-scale physics. In Jeffreson & Kruijssen (2018), we developed a theory for the cloud lifetime, dependent upon the large-scale dynamics of the galactic environment. Applied to the CMZ, our theory can be used to quantitatively predict the cloud lifetime and to understand the role played by galactic dynamics in cloud evolution and subsequent star formation. In this paper, we combine the analytic theory of Jeffreson & Kruijssen (2018) with the model of Krumholz et al. (2017). We determine which large-scale dynamical processes are most important in setting the course of cloud evolution, and consequently star formation, in the gas inflow from radii of $\sim$ 500 pc down to the 100-pc stream. This not only gives a quantitative prediction for the variation in cloud lifetime with radius, but also divides the CMZ into dynamical regimes, in which cloud evolution is dominated by different dynamical processes. The dynamically-driven gas flows described in Krumholz et al. (2017) must pass through each of these dynamical regimes on their way towards the central SMBH.

⋆ s.jeffreson@uni-heidelberg.de

© 2017 The Authors

Table 1. The dynamical time-scales used in the cloud lifetime theory of Jeffreson & Kruijssen (2018) and their physical interpretations.

Time-scale	Symbol	Physical meaning	Analytic form	Physical variables
τ_κ	κ	Time-scale for the effect of epicyclic perturbations on GMCs.	$\frac{4\pi}{\Omega\sqrt{2(1+\beta)}}\frac{1}{\sqrt{3+\beta}}$	Ω, β
$\tau_{\rm ff,g}$	f	Time-scale for the gravitational collapse of the ISM on approximately sub-Toomre length scales, as in Krumholz et al. (2012).	$\sqrt{\frac{3\pi^2}{32\phi_P(1+\beta)}}\frac{Q}{\Omega}$	Q, Ω, β, ϕ_P
$\tau_{\rm cc}$	c	Time-scale for collisions between GMCs (Tan 2000).	$\frac{2\pi Q}{9.4 f_G \Omega(1+0.3\beta)(1-\beta)}$	Q, Ω, β
τ_β	β	Time-scale on which galactic shear pulls a cloud apart in the azimuthal direction. This is the only time-scale that has a fundamentally dispersive effect on molecular clouds. As such, the rate of galactic shear τ_β^{-1} is *subtracted* from the other rates in Equation 1.	$\frac{2}{\Omega(1-\beta)}$	Ω, β

2 THEORY

In Jeffreson & Kruijssen (2018), we introduced a theory for the molecular cloud lifetime, dependent upon the large-scale dynamics of the interstellar medium (ISM). Here we develop the salient points of this theory in relation to the central 500 pc of the Milky Way. For a more detailed overview of the theory, we refer the reader to Jeffreson & Kruijssen (2018).

Our theory of the molecular cloud lifetime is independent of the size, structure and gravitational boundedness of molecular clouds, in accordance with the diverse range of objects that can observationally be classified as GMCs. It calculates the cloud lifetime as an environmentally-dependent quantity, consistent with the observed environmental dependence of the star formation efficiency per unit time in spiral and dwarf galaxies (Leroy et al. 2008). Using only the observable properties of the ISM, the cloud lifetime τ in the CMZ can be quantified by adding the rates of the relevant large-scale dynamical processes in parallel, such that

$$\tau = |(\tau_\kappa^{-1} + \tau_{\rm ff,g}^{-1} + \tau_{\rm cc}^{-1} - \tau_\beta^{-1})|^{-1}. \quad (1)$$

The different time-scales in this equation and their physical variables are summarised in Table 1, where Ω is the angular velocity of the midplane ISM, β is the galactic shear parameter

$$\beta = \frac{{\rm d}\ln v_c}{{\rm d}\ln R}, \quad (2)$$

for circular velocity $v_c(R)$ at galactocentric radius R, and Q is the Toomre (1964) Q parameter for the ISM midplane gas

$$Q = \frac{\kappa\sigma_g}{\pi G \Sigma_g}, \quad (3)$$

for an epicyclic frequency κ, midplane gas velocity dispersion σ_g, and midplane gas surface density Σ_g. The variable ϕ_P quantifies the contribution of the stellar potential to the ISM pressure, as defined in Elmegreen (1989),

$$\phi_P = 1 + \frac{\Sigma_s}{\Sigma_g}\frac{\sigma_g}{\sigma_s}, \quad (4)$$

where σ_s and Σ_s refer to the stellar velocity dispersion and surface density, respectively. The variable $f_G = 0.5$ in $\tau_{\rm cc}$ is a 'collision probability' parameter defined and fitted to observations in Tan (2000). All time-scales depend inversely on the angular velocity Ω, such that the normalised cloud lifetime τ/Ω^{-1} is described within a parameter space spanned by the four physical variables β, Q, ϕ_P and f_G. Of these, we fix f_G to its above fiducial value, and note that only the time-scale $\tau_{\rm ff,g}$ for gravitational free-fall depends weakly on ϕ_P. The cloud lifetime therefore varies within a fundamental parameter space spanned by β, Q and Ω, with a secondary dependence on ϕ_P. Values of these variables for the CMZ are accessible through measurements of its rotation curve, velocity dispersion profile, and surface density profile. Since neither the Galactic bar nor the Galactic spiral arms extend down to the maximum galactocentric radius of ~ 500 pc considered here, we have excluded the dynamical time-scale $\tau_{\Omega_{\rm P}}$ for spiral-arm crossings, although it is discussed in Jeffreson & Kruijssen (2018).

3 APPLICATION TO THE CMZ

In order to use Equation 1 to calculate the cloud lifetime in the CMZ, we require its rotation curve, velocity dispersion profile and surface density profile. The accurate measurement of velocity dispersions in the CMZ is currently an active topic of research (Shetty et al. 2012; Henshaw et al. 2016a,b), while the edge-on CMZ viewing angle prohibits the acquisition of an accurate face-on surface density profile. As such, we use observational data for the rotation curve of the CMZ from Launhardt et al. (2002), but use the gas velocity dispersions and gas surface densities produced by simulation run m10r050f10 from the dynamical model of Krumholz et al. (2017), which are consistent with the gas properties inferred observationally for the CMZ (see e.g. their Figures 10 and 14 and compare to Kruijssen et al. 2014; Henshaw et al. 2016a,b). This numerical simulation successfully reproduces several of the observed properties of the CMZ, in particular the large-scale gas distribution.

In Figure 1, we display the time-scales of each cloud evolutionary mechanism (top panel) and the resulting cloud lifetimes (bottom panel) as a function of galactocentric radius, at a simulation time of 485 Myr in the model m10r050f10, corresponding to the gas properties that best match those observed at the current epoch. We also display the standard deviation in each quantity at each radius over the whole range of model parameters during the most recent 100 Myr in Krumholz et al. (2017), to provide an indication of how much they vary.[1] The value of ϕ_P has been calculated at each galactocentric radius using the stellar velocity dispersion of $\sigma_{\rm s} \approx 100$ kms^{-1} from de Zeeuw (1993), the rotation curve from Launhardt et al. (2002), and the gas surface density and velocity dispersion profiles from Krumholz et al. (2017). As in Jeffreson & Kruijssen (2018), we indicate *regions of relevance*, enclosed by black dashed lines. The *relevance* of a single cloud evolutionary mechanism depends on the ratio of its time-scale to the minimum evolutionary time-scale $\tau_{\rm min}$ (where $\tau < \tau_{\rm min}$), or to the cloud lifetime τ (where $\tau > \tau_{\rm min}$ due to shear support). If this ratio exceeds a value of 2, i.e. the mechanism occurs at under half the rate of the dominant evolutionary mechanism for $\tau < \tau_{\rm min}$, or at under half the rate of cloud destruction for $\tau > \tau_{\rm min}$, then its effect on cloud evolution is deemed *irrelevant*.

We find that the CMZ can be divided into two distinct regimes,

[1] The standard deviation is computed by sampling the last 100 Myr of evolution at 5 Myr intervals for the models m01r050f10, m03r025f10, m03r050f05, m03r050f10, m03r050f20 and m10r050f10.

corresponding to the grey- and white-shaded areas in the bottom panel of Figure 1. The grey-shaded areas ($R \gtrsim 120$ pc and $R \lesssim 45$ pc) indicate the galactocentric radii that are dominated by galactic shear, to the extent that the rate of shearing outpaces the combined rates of all dynamically-compressive cloud evolutionary mechanisms ($\tau_\beta^{-1} > \tau_\kappa^{-1} + \tau_{\rm ff,g}^{-1} + \tau_{\rm cc}^{-1}$). The white-shaded area ($45 \lesssim R/\mathrm{pc} \lesssim 120$) indicates the radii that are dominated by dynamically-compressive mechanisms of cloud evolution. Due to the extremely low gas column density at galactocentric radii $R \lesssim 45$ pc, we will ignore the innermost grey-shaded area from hereon. We will identify the shear-dominated regime with the outer CMZ (labelled 'A') and will identify the dynamically-compressive regime with the radii close to the 100-pc stream (labelled 'B').

In the vicinity of the 100-pc stream ('B', $45 \lesssim R \lesssim 120$ pc in Figure 1), the majority of GMCs are expected to collapse and form stars, due to the dominance of dynamically-compressive cloud evolutionary mechanisms. At radii from 50 to 110 pc, gravitational free-fall 'f' is the only relevant mechanism of cloud evolution, leading to short cloud lifetimes between 0.3 and 5 Myr at the current epoch. The only exception to the dominance of gravity arises at the entrance to the 100-pc stream at ~ 120 pc, where the volume density of gas entering the star-forming ring is still low enough that epicyclic perturbations and galactic shear compete with gravitational free-fall (note the equality of all time-scales at ~ 120 pc in the top panel of Figure 1). The importance of epicyclic perturbations at ~ 120 pc is consistent with the hypothesis that star formation in the ~ 100 pc stream may be triggered by tidal compressions due to pericentre passages of molecular clouds on epicyclic orbits (Longmore et al. 2013b; Kruijssen et al. 2015; Henshaw et al. 2016b). In the outer CMZ 'A', cloud lifetimes are consistently longer, around 10 Myr, due to the increased degree of shear support, which balances closely with the dynamically-compressive mechanisms of cloud evolution. At these radii, self-gravity is irrelevant and thus cloud evolution is controlled by shear and epicyclic perturbations, '$\beta\kappa$'. We expect the majority of GMCs in the outer CMZ to have low star formation efficiencies per unit mass, and eventually to be dispersed by galactic shear.

As indicated by the standard deviations in $\tau_{\rm ff,g}$, $\tau_{\rm cc}$ and the cloud lifetime τ, the results do not vary much over the past 100 Myr (despite considerable variations in the SFR), nor do they depend strongly on the parameter choices of the Krumholz et al. (2017) model. That is, gravitational free-fall always dominates in the vicinity of the 100-pc stream, and a combination of galactic shear and epicyclic perturbations dominate elsewhere. The cloud lifetimes themselves vary by 3 per cent at ~ 200 pc (region A) and by up to 30 per cent at ~ 100 pc (region B), which corresponds to a shift from 0.3 to 0.2 Myr in the minimum cloud lifetime for region B. The major downward uncertainty between 120–150 pc arises because region B extends to ~ 150 pc in a small subset of the complete range of models considered.

In the bottom panel of Figure 1, we also include the feedback-adjusted cloud lifetime. In the model of Jeffreson & Kruijssen (2018), we assume that the lifetime of a cloud is determined by its evolution towards star formation, and that destruction by feedback occurs on a much shorter time-scale. This assumption is appropriate for galactic discs, where the dynamical time-scales generally greatly exceed the time-scale for gas removal by feedback, but breaks down in the 100-pc stream, where the dynamical time-scales are short. We thus add a feedback time-scale of $\tau_{\rm fb} = 1.1$ Myr to the calculated cloud lifetime, which corresponds to the time taken to traverse the section of the 100-pc stream between Sgr B2, where stellar feedback first sets in, and Sgr B1, where the most of the

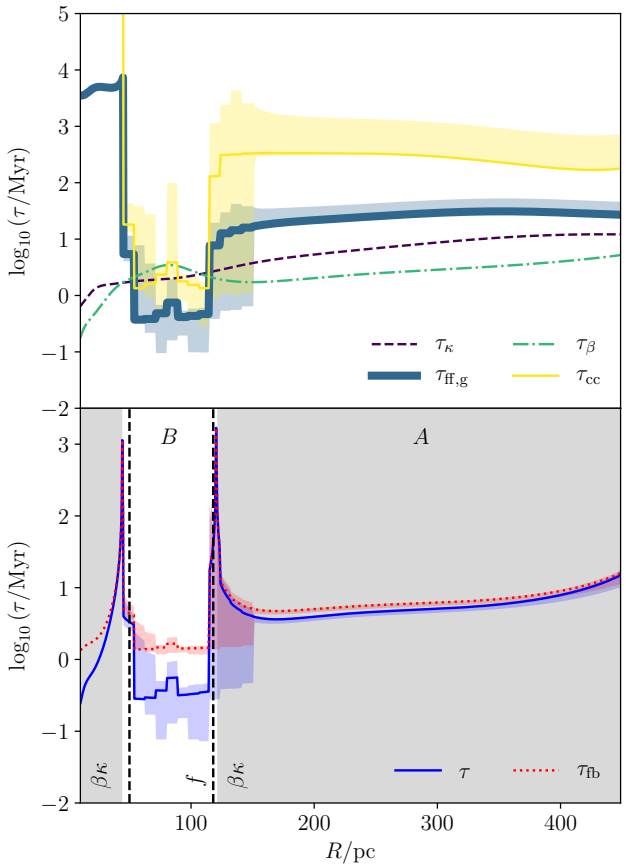


Figure 1. Values of the cloud lifetime predicted by our model for the current gas distribution in the best-matching simulation of Krumholz et al. (2017), including the standard deviation in the model-dependent time-scales across the last 100 Myr of all models (see the text). The upper panel gives each of the time-scales of dynamical evolution. The blue solid line in the lower panel gives the lifetime calculated using Equation 1, and the red dotted line adds a feedback time-scale $\tau_{\rm fb} \sim 1.1$ Myr to this lifetime (see the text). The grey shaded areas indicate the galactocentric radii at which the rate of galactic shear τ_β^{-1} is higher than the combined rates of all other mechanisms, while the black dashed vertical lines delineate the *regions of relevance*, discussed in Section 3 and labelled according to Table 1. The labels 'A' and 'B' refer to the outer CMZ and the vicinity of the 100-pc stream, respectively.

molecular gas has been blown out (Kruijssen et al. 2015; Barnes et al. 2017). With the addition of this feedback time-scale, the range of cloud lifetimes predicted for the 100-pc stream is raised to 1.4–3.9 Myr. We emphasise that the feedback time-scale is the only result in this paper that depends on an evolutionary progression of cloud evolution along the 100-pc stream, from Sgr B2 to Sgr B1.

In Figure 2, we show the CMZ model by Krumholz et al. (2017) in the fundamental parameter space (β, Q), over which the normalised cloud lifetime, τ/Ω^{-1}, varies. Triangular points denote the data at the current epoch, corresponding to the cloud lifetimes in Figure 1. Circular points denote the data at all other epochs. The values of β are taken from the observed rotation curve, which is assumed to be constant in time, and the *regions of relevance* are delineated by black dashed lines. The shear-dominated regime 's', corresponding to the grey-shaded regions in Figure 1, is separated by a white solid line from the dynamically-compressive regime 'c'. We set $\phi_P \sim 1$, the value appropriate to the 100-pc stream (c.f. de Zeeuw 1993; Launhardt et al. 2002; Krumholz et al. 2017), be-

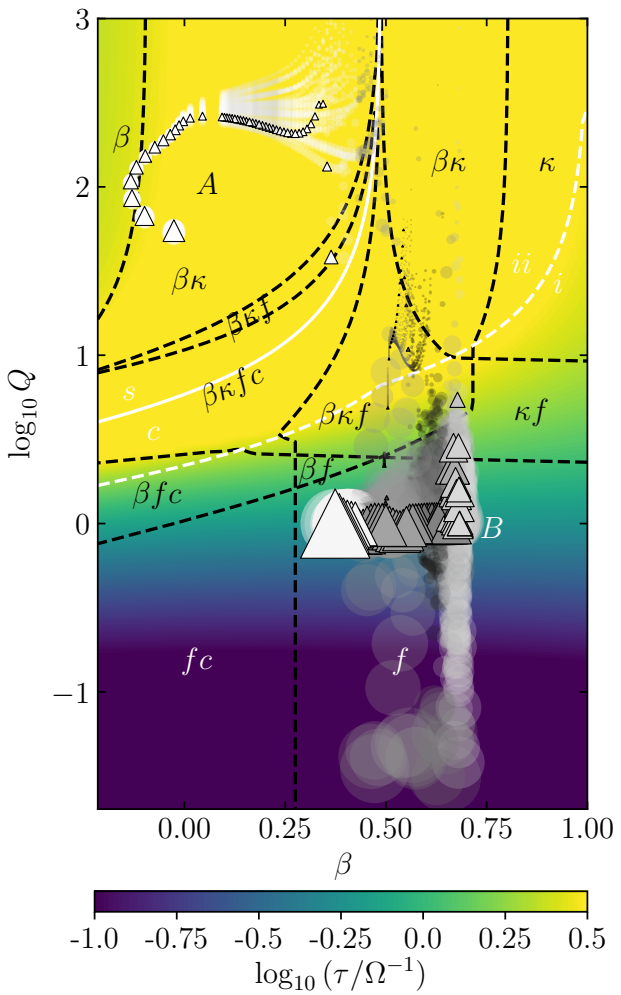


Figure 2. Values of the predicted cloud lifetime in units of angular velocity Ω (coloured contours) for a cross-section of $(\beta, \log Q)$ parameter space with $\phi_P \sim 1$, overlaid with values of β and $\log Q$ (translucent circles) for the CMZ, at 10 Myr intervals from 100 to 500 Myr in the best-matching simulation of Krumholz et al. (2017). The data at 485 Myr (the current epoch) are given by triangles. The data points are colour-coded on a grey scale between black and white by galactocentric radius, where a lighter colour corresponds to a larger radius. Their area is weighted on a linear scale by the total gas mass in each radial interval, where the largest data points represent the largest quantities of molecular gas. The dashed black lines enclose the *regions of relevance* for each time-scale, labelled as in Figure 1. The dashed white lines divide the regimes 'ii' in which the cloud lifetime is longer than the minimum evolutionary time-scale from the regimes 'i' in which it is shorter. The solid white lines divide the shear-dominated regime 's' from the dynamically-compressive regime 'c' (grey- and white-shaded regions, respectively, in Figure 1). The labels 'A' and 'B' denote the regions of the CMZ shown in Figure 1 and discussed in Section 3.

cause it only affects $\tau_{\rm ff,g}$ and the effect of gravitational free-fall is strongest in the 100-pc stream. We note that higher values of $12 \lesssim \phi_P \lesssim 100$, appropriate to radii of 120–500 pc, do not significantly alter the predicted cloud lifetime outside the 100-pc stream.

We find that the two distinct regimes 'A' and 'B', corresponding to different galactocentric radii in Figure 1, are also distinct in (β, Q, Ω) parameter space. The outer ('A', $\gtrsim$ 120 pc) region of the CMZ, through which gas flows inwards with large scale heights and low volume densities, is characterised by an approximately-flat rotation curve and very high levels of gravitational stability ($\beta < 0.5$ and $Q \gtrsim 60$). According to the model of Krumholz et al. (2017), 'A' can be interpreted as a body of gas spiralling in towards the star-forming, ring-shaped stream 'B' at $\sim$ 100 pc, propelled by shear-driven acoustic instabilities. Due to high levels of shearing and gravitational stability, GMCs in the outer CMZ fall exclusively in the dynamically-dispersive regime 's' of parameter space, and are governed by a combination of galactic shear and epicyclic perturbations '$\beta\kappa$'. The competition between dynamically-compressive and dynamically-dispersive mechanisms of cloud evolution in this regime elongates the cloud lifetime to between 2.3 and 3.3 orbital times $1/\Omega$. Note that we have excluded $> 3\sigma$ outliers for this and all subsequent ranges, in order to reflect the typical cloud lifetime at each interval of galactocentric radii.

In the vicinity of the 100-pc stream 'B', between galactocentric radii of 45 and 120 pc, the gas inflow stalls due to a local shear minimum in the rotation curve (Krumholz & Kruijssen 2015), where $0.5 \lesssim \beta \lesssim 0.75$. It condenses to small scale heights ($\sim$ 3 pc) and high volume densities ($\sim$ 500 $M_\odot {\rm pc}^{-3}$), such that the level of gravitational stability falls as low as $Q \sim 0.1$. At these radii, we expect that the majority of GMCs are governed by gravity alone (in regime 'f' of parameter space), and are therefore destroyed by gravitational collapse and the subsequent stellar feedback. In particular, we expect cloud lifetimes on the outside of the 100-pc stream (between 100 and 120 pc, corresponding to the lighter-coloured data points in region 'B') to be very short ($\sim$ 1 orbital time $1/\Omega$). On the inside of the stream (between 45 and 100 pc, corresponding to the darker-coloured points in region 'B'), the molecular gas surface density is depleted by star formation (Krumholz et al. 2017), leading to gas masses as low as one 1000th of the mass on the outside of the stream (compare the areas of the dark- and light-coloured data points in region 'B' of Figure 2). Due to its low gas fraction, this remaining material has a high degree of gravitational stability, leading to longer cloud lifetimes (between 1 and 3 orbital times).

The molecular gas that survives the star-forming ring exits the local shear minimum and makes its way towards the nuclear cluster and eventually the central SMBH (Krumholz et al. 2017). This inner region of the CMZ is not shown in Figure 2, because the vast majority of molecular gas in the Krumholz et al. (2017) model is either consumed by star formation or blown out by feedback at earlier times in the star-forming ring, producing unreliable values of Q at $\lesssim$ 45 pc. However, we do expect that the cloud lifecycle in the inner CMZ ($R \lesssim 45$ pc) is controlled by similar mechanisms as in the outer CMZ 'A' due to its flat ($\beta < 0.5$) rotation curve, but with higher levels of gravitational stability due to its even lower gas density.

Comparing the triangular (current, quiescent phase) and circular (all snapshots) data points in Figure 2, it is clear that there is little time-variation of the parameters β and Q between the starburst and quiescent phases of the Krumholz et al. (2017) model, resulting in CMZ cloud lifetimes that are also relatively time-invariant. Over a period of $\sim$ 500 Myr in simulation time, the radial extent of the gravity-dominated regime 'c' and the radial extents of each region of relevance are constant to within 10 per cent. This is a direct result of the shape of the gravitational potential and, hence, the rotation curve. As the CMZ evolves, the time-scales on which gravity-dominated clouds are destroyed by collapse and feedback in the 100-pc stream 'B', and on which shear-dominated clouds are dispersed by galactic shear outside the 100-pc stream 'A', is relatively constant. The most notable exception to time-invariance occurs in the vicinity of the 100-pc stream 'B', where a sharp drop in the cloud lifetime occurs during each starburst phase, corresponding to the scatter of points down to $Q \sim 0.1$ in regime 'f' of Fig-

ure 2. This is due to the simultaneous drop in the turbulent velocity dispersion and the rise in the molecular gas surface density that accompanies a starburst, producing a sudden drop in Toomre Q.

Although gravitational free-fall is the only relevant cloud evolutionary mechanism throughout the majority of the 100-pc stream (see regime 'f' of Figure 2) a number of data points are also located in regimes 'κf' and '$\beta\kappa f$', where we expect epicyclic perturbations to have a significant influence on cloud evolution. This is consistent with the hypothesis that tidal compressions may trigger cloud collapse and star formation in the 100-pc stream, due to pericentre passages of molecular clouds on eccentric orbits, or by accretion onto the stream (Longmore et al. 2013b; Kruijssen et al. 2018).

We may estimate the fraction of clouds whose collapse is triggered by epicycles, by first calculating the fraction of clouds $N(R)$ that survive until they reach galactocentric radius R in the gravity-dominated regime 'c' (i.e. in the vicinity of the 100-pc stream). This is given by the differential equation

$$v_R \frac{\mathrm{d}N(R)}{\mathrm{d}R} = -\tau^{-1}(R)N(R), \tag{5}$$

where v_R is the radial inflow velocity, calculated self-consistently at each radius in the model of Krumholz et al. (2017), and $\tau^{-1}(R)$ is the rate of cloud destruction, as calculated in Equation (1). Solving this equation numerically for $N(R)$, we find that at the current epoch, 100 per cent of clouds are destroyed between $R = 120$ pc and $R = 115$ pc, at the very outer edge of the gravity-dominated regime. That is, the inflow velocity of the clouds drops significantly as they spiral inwards towards the local shear minimum, so that all are destroyed before their apocentric radii shrink from 120 to 115 pc. This demonstrates that the groups of darker-coloured points (indicating smaller radii) in regimes 'κf' and '$\beta\kappa f$' of Figure 2 do not give meaningful information about the course of cloud evolution: for radii close to 45 pc, very few molecular clouds remain.

Of the clouds that are destroyed in each interval of galactocentric radius, we may estimate the statistical fraction $F(R)$ of cloud destruction through star formation and feedback that is driven by epicycles, i.e. the fraction of star formation events that is driven by pericentre passages. This is defined to exclude cloud dispersal by shear and (in regime 'c' of parameter space) is given by

$$F(R) = \frac{\tau_\kappa^{-1}}{\tau_\kappa^{-1} + \tau_{\mathrm{ff,g}}^{-1} + \tau_{\mathrm{cc}}^{-1}}, \tag{6}$$

The overall fraction of clouds F that are destroyed by epicycles is then given by the product of $F(R)$ and the fraction of clouds destroyed between R and $R + \Delta R$, summed over all radii, so that

$$F = \sum_R [N(R + \Delta R) - N(R)]F(R) \approx 0.2, \tag{7}$$

at the current epoch. That is, 20 per cent of cloud destruction, upon accretion onto the 100-pc stream, is caused by epicyclic perturbations (i.e. pericentre passages). Across the full duty cycle at times close to the current epoch, the fraction of cloud destruction caused by epicyclic perturbations does not vary significantly and remains (with mostly downward variations) in the range 10–30 per cent.

4 CONCLUSIONS

Using the theoretical output of Krumholz et al. (2017), along with the observed rotation curve in the CMZ of the Milky Way, we have applied the theory of cloud lifetimes presented in Jeffreson & Kruijssen (2018) to the Galactic centre.

From a cloud evolutionary perspective, we find that the CMZ is divisible into two dynamical regimes. At galactocentric radii from $\sim$ 120-500 pc, the cloud lifecycle is primarily dominated by galactic shear, to the extent that the rate of shearing is faster than the combined rates of all other cloud evolutionary mechanisms. At these galactocentric radii we expect clouds to be sheared apart on time-scales between 3 and 9 Myr, before collapse and star formation can occur, leading to low star formation efficiencies. Conversely, at galactocentric radii from $\sim$ 45-120 pc, we expect to find clouds that collapse and form stars on much shorter time-scales, with median lifetimes between $\sim$ 0.3 and 2.8 Myr. If we lift the assumption of instantaneous stellar feedback and include a gas removal time-scale of $\tau_{\mathrm{fb}} = 1.1$ Myr, motivated by observations, this range of cloud lifetimes becomes 1.4–3.9 Myr.

At the outer edge of the 100-pc stream, the time-scale for epicyclic perturbations, which quantifies the influence of orbital eccentricity on the cloud lifecycle, obtains equality with the free-fall time-scale. This result is consistent with the hypothesis of tidally-triggered collapse in the 100-pc stream, as initially proposed by Longmore et al. (2013b) and later expanded by Kruijssen et al. (2015) and Henshaw et al. (2016b). While the similarity of the free-fall and epicyclic time-scales implies that some accreting gas streams may collapse due to a tidal compression at pericentre (in approximately 20 per cent of cases), it also means that some gas streams may undergo free-fall collapse due to their arrival on the 100-pc stream, before pericentre is reached (in around 80 per cent of cases). This simple time-scale argument corroborates the numerical simulations presented by Kruijssen et al. (2018), who show that the compressive tidal field at the radii of the 100-pc stream may have an equal, if not stronger effect on cloud evolution than the pericentre passage. Since the gas is flowing in from larger radii, both collapse mechanisms lead to an evolutionary progression of star formation, either post-pericentre, or after their moment of accretion onto the 100-pc stream. In combination with the known orbits of the CMZ gas streams, this provides an absolute evolutionary timeline that allows the cloud lifetimes predicted here to be directly tested with currently available observations.

ACKNOWLEDGEMENTS

SMRJ and JMDK acknowledge funding from the German Research Foundation (DFG) in the form of an Emmy Noether Research Group (grant number KR4801/1-1). JMDK acknowledges support from the European Research Council (ERC) under the European Union's Horizon 2020 research and innovation programme via the ERC Starting Grant MUSTANG (grant number 714907). MRK acknowledges support from the Australian Research Councils Discovery Projects funding scheme (project DP160100695). We thank an anonymous referee for a constructive report, which improved the paper.

REFERENCES

Barnes A. T., Longmore S. N., Battersby C., Bally J., Kruijssen J. M. D., Henshaw J. D., Walker D. L., 2017, MNRAS, 469, 2263
Elmegreen B. G., 1989, ApJ, 338, 178
Ferrière K., Gillard W., Jean P., 2007, A&A, 467, 611
Henshaw J. D., et al., 2016a, MNRAS, 457, 2675
Henshaw J. D., Longmore S. N., Kruijssen J. M. D., 2016b, MNRAS, 463, L122
Immer K., Schuller F., Omont A., Menten K. M., 2012, A&A, 537, A121
Jeffreson S. M. R., Kruijssen J. M. D., 2018, MNRAS submitted

Kauffmann J., Pillai T., Zhang Q., 2013, ApJ, 765, L35
Kennicutt R. C., Evans N. J., 2012, ARA&A, 50, 531
Kruijssen J. M. D., Longmore S. N., 2013, MNRAS, 435, 2598
Kruijssen J. M. D., Longmore S. N., Elmegreen B. G., Murray N., Bally J., Testi L., Kennicutt R. C., 2014, MNRAS, 440, 3370
Kruijssen J. M. D., Dale J. E., Longmore S. N., 2015, MNRAS, 447, 1059
Kruijssen J. M. D., et al., 2018, MNRAS to be submitted
Krumholz M. R., Kruijssen J. M. D., 2015, MNRAS, 453, 739
Krumholz M. R., Dekel A., McKee C. F., 2012, ApJ, 745, 69
Krumholz M. R., Kruijssen J. M. D., Crocker R. M., 2017, MNRAS, 466, 1213
Launhardt R., Zylka R., Mezger P. G., 2002, A&A, 384, 112
Leroy A. K., Walter F., Brinks E., Bigiel F., de Blok W. J. G., Madore B., Thornley M. D., 2008, AJ, 136, 2782
Longmore S. N., et al., 2013a, MNRAS, 429, 987
Longmore S. N., et al., 2013b, MNRAS, 433, L15
Oka T., Hasegawa T., Sato F., Tsuboi M., Miyazaki A., Sugimoto M., 2001, ApJ, 562, 348
Rathborne J. M., et al., 2014, ApJ, 786, 140
Shetty R., Beaumont C. N., Burton M. G., Kelly B. C., Klessen R. S., 2012, MNRAS, 425, 720
Tan J. C., 2000, ApJ, 536, 173
Toomre A., 1964, ApJ, 139, 1217
Yusef-Zadeh F., et al., 2009, ApJ, 702, 178
de Zeeuw T., 1993, in Dejonghe H., Habing H. J., eds, IAU Symposium Vol. 153, Galactic Bulges. p. 191

This paper has been typeset from a TEX/LATEX file prepared by the author.